Research Square

Preprints are preliminary reports that have not undergone peer review.
They should not be considered conclusive, used to inform clinical practice,
or referenced by the media as validated information.

Enhanced recombinant production of the antimicrobial peptide CRAMP-34 in Pichia pastoris through fermentation optimization and characterization of its antibacterial and stability properties

Fan Wang
Southwest University
Haoyuan Yan
Southwest University
Siping Yang
Southwest University
Chengjun Ma
China Pharmaceutical University
Rong Li
Southwest University
Shuting Liu
Southwest University
Xintong Ren
Southwest University
Jinhong Deng
Southwest University
Wei Wei
Southwest University
Hongzao Yang
Southwest University
Hongwei Chen
dyxchw@swu.edu.cn
Southwest University

Research Article

Keywords: Antimicrobial peptides, biofilm, Komagataella phaffii, recombinant expression, membrane permeabilization

Posted Date: November 12th, 2026

DOI: https://doi.org/10.21203/rs.3.rs-11402519/v1

License: This work is licensed under a Creative Commons Attribution 4.0 International License.
Read Full License

Additional Declarations: No competing interests reported.

Enhanced recombinant production of the antimicrobial peptide CRAMP-34 in *Pichia pastoris* through fermentation optimization and characterization of its antibacterial and stability properties

Abstract

Antimicrobial peptides are promising alternatives to conventional antibiotics, but their application is limited by inefficient recombinant production. This study established an efficient *Pichia pastoris* platform for producing mouse-derived CRAMP-34 and evaluated its antibacterial properties. The codon-optimized CRAMP-34 gene was integrated into pPIC9K, and a high-copy *P. pastoris* GS115 transformant was obtained by G418 screening. Induction conditions were optimized through single-factor experiments and L9 orthogonal design, reaching a maximum freeze-dried product yield of 5.66% at 24°C with 3.0% methanol added every 24h for 144h; the optimum was confirmed in parallel experiments. Recombinant CRAMP-34 demonstrated strong antibacterial activity against *Escherichia coli*, accompanied by inhibition of biofilm formation and disruption of preformed biofilms. Concentration-dependent increases in bacterial membrane permeability and plasmid DNA binding were observed, indicating that membrane disruption and DNA interaction contributed to the antibacterial activity of CRAMP-34. CRAMP-34 also showed good tolerance to heat, salts, freeze-thaw cycles, and pepsin digestion, although its activity was reduced by trypsin and high-dose papain. These findings establish an efficient production strategy and support CRAMP-34 as a promising antimicrobial agent.

Keywords

Antimicrobial peptides; biofilm; *Komagataella phaffii*; recombinant expression; membrane permeabilization

1. Introduction

The rapid emergence of multidrug-resistant bacteria has created an urgent need for new classes of antimicrobials, and antimicrobial peptides (AMPs) have attracted considerable attention as one of the most promising alternatives to conventional antibiotics (Talapko et al. 2022). AMPs are small, cationic and amphipathic molecules that kill microorganisms primarily by disrupting the cytoplasmic membrane, a mode of action that makes the development of resistance less likely than for conventional antibiotics (Wang et al. 2024). The problem is compounded by bacterial biofilms, which are intrinsically tolerant to many antibiotics and are responsible for a large proportion of chronic and device-associated infections; compounds that combine direct antibacterial activity with anti-biofilm action are therefore highly desirable (Luo and Song 2021; Pontes et al. 2022). Among the major AMP families, cathelicidins are a group of multifunctional host-defense peptides widely distributed in vertebrates; CRAMP (cathelin-related antimicrobial peptide) is the principal cathelicidin of the mouse (Xie et al. 2020; Zhang et al. 2019). Based on the sequence of the murine peptide CRAMP, we designed CRAMP-34, a 34-residue cationic peptide predicted to adopt an amphipathic α-helix and to carry a net positive charge-features considered favourable for antimicrobial activity (Bhattacharjya et al. 2024; Zeth and Sancho-Vaello 2021).

Despite their therapeutic potential, the practical application of AMPs is largely restricted by the high cost of chemical synthesis and the low yields of natural extraction (Roca-Pinilla et al. 2022; Zhang 2025). Recombinant expression in the methylotrophic yeast *Pichia pastoris (syn. Komagataella phaffii)* provides an attractive alternative because of its strong methanol-inducible AOX1 promoter, efficient protein secretion, eukaryotic post-translational modifications and inexpensive culture media (Barone et al. 2023; Mohammadzadeh et al. 2021). Many AMPs, including plectasin and hybrid peptides such as cecropin A-magainin 2 and cecropin-melittin derivatives, have been successfully produced in *P. pastoris* (Dong et al. 2023). However, the yield and biological activity of recombinant AMPs depend strongly on the induction conditions, including temperature, methanol concentration and induction time, and the reported optima vary considerably among peptides (Bustos et al. 2022;

Garrigós-Martínez et al. 2021). In addition to efficacy, the therapeutic applicability of AMPs depends on their selectivity for bacterial over host-cell membranes, for which hemolytic activity serves as a first-line in vitro indicator (Svensson and Nilsson 2025).

In the present study, the CRAMP-34 gene was codon-optimized and expressed in *P. pastoris* GS115, and the induction conditions were optimized by single-factor experiments combined with an L9(3^4) orthogonal design. The antibacterial spectrum, minimum inhibitory concentration (MIC), effects on bacterial growth and biofilm formation, membrane permeability, DNA-binding activity, hemolytic activity and stability of the recombinant peptide were then characterized, providing a basis for the scaled production and further development of CRAMP-34.

2. Materials and methods

2.1. Strains, plasmids and reagents

P. pastoris GS115 and the expression vector pPIC9K were used for protein production. The CRAMP-34 gene was codon-optimized with the online tool ExpOptimizer and synthesized by Tsingke Biotechnology Co., Ltd. (Chongqing, China). *Escherichia coli DH5α* was used for plasmid propagation. *Staphylococcus aureus ATCC 25923*, *Pseudomonas aeruginosa ATCC 27853*,*Pseudomonas aeruginosa* strain *PAO1*, *E. coli ATCC 25922*, *Acinetobacter lwoffii* and *Bacillus subtilis* were used for antibacterial assays, and *E. coli* strain *Ec032* was used in the growth-curve, biofilm and mechanism assays. SacI, T4 DNA ligase, DNA markers and the plasmid extraction kit were purchased from Takara Bio (Beijing, China). Yeast extract, peptone, YNB, G418 and other analytical-grade reagents were obtained from commercial suppliers.

2.2. Vector construction and transformation

The synthesized CRAMP-34 gene was cloned into pPIC9K to generate the recombinant expression vector pPIC9K-CRAMP-34. The plasmid was propagated in *E. coli DH5α* on LB agar containing 30μg/mL kanamycin, extracted with a plasmid purification kit and verified by PCR and restriction analysis. The verified plasmid was linearized with SacI (37°C, overnight), purified by agarose gel electrophoresis and transformed into *P. pastoris* GS115 competent cells by the heat-shock method.

Transformants were first selected on MD plates (30°C, 72h). To screen for high-copy integrants, well-grown single colonies were transferred to YPD plates containing 0.25, 0.5, 0.75, 1.0, 1.5, 1.75, 2.0, 3.0 and 4.0 mg/mL G418 and incubated at 30°C for 72-96 h. Clones growing on 3.0 mg/mL G418 were further confirmed by colony PCR with the AOX1 primers (AOX1-F/AOX1-R), using the empty vector as a negative control, to exclude false-positive transformants(Mohammadzadeh et al. 2021).

2.3. Optimization of CRAMP-34 expression

A single colony of a high-copy transformant was cultured overnight in YPD at 30°C and 250 rpm, transferred to BMGY medium and grown at 30°C and 250 rpm for 18-24 h until the OD600 reached 1.0-1.4. Cells were harvested, washed twice with PBS, resuspended in BMMY medium and induced at 250 rpm. In single-factor experiments, one parameter was varied while the others were held constant: induction temperature (22, 24, 26, 28, 30 or 32°C with 2.0% methanol added every 24h for 72h), methanol concentration (0.5, 1.0, 1.5, 2.0, 2.5 or 3.0% (v/v) added every 24 h at 28°C for 72h) or induction time (24, 48, 72, 96, 120 or 144 h at 28°C with 2.0% methanol). The antibacterial activity of the culture supernatant, expressed as the inhibition zone diameter against *S. aureus*, was used as the readout to define the optimum range of each factor.

Based on the single-factor results, an L9(3^4) orthogonal design was established with three factors at three levels: temperature (24, 26, 28°C), methanol concentration (2.0, 2.5, 3.0%) and induction time (96, 120, 144h). The comprehensive score for each run combined the inhibition zone diameters against *S. aureus* and *P. aeruginosa*, the protein concentration of the supernatant and the eradication rate of mature *P. aeruginosa* biofilms. Range analysis and analysis of variance (ANOVA) were performed, and the optimal combination was validated by three parallel experiments(Garrigós-Martínez et al. 2021).

2.4. Freeze-drying, protein determination and Tricine-SDS-PAGE

After optimal induction, the culture supernatant was centrifuged, filtered through 0.22μm membranes, dispensed into tubes, frozen at -80°C overnight and lyophilized for 96 h. The freeze-

dried powder was weighed, and the product yield was calculated as the mass of powder obtained per volume of supernatant.For protein identification, the culture supernatant was analyzed by Tricine-SDS-PAGE using a three-gel system (stacking, spacer, and separating gels) optimized for small peptides. Proteins were visualized by Coomassie Brilliant Blue R-250 staining after fixation and destaining.

2.5. Antibacterial activity and minimum inhibitory concentration

Antibacterial activity was measured by the agar well diffusion method. Bacterial suspensions (1×10^6 CFU/mL) were spread on solidified LB agar plates, wells were punched in the agar, and 100μL of culture supernatant was added to each well; supernatant from the empty-vector strain served as the negative control and ampicillin as the positive control. Plates were incubated at 37°C for 12-18 h and the inhibition zone diameters were measured.

For MIC determination, 1.024g of the freeze-dried powder was dissolved in 2mL of sterile water and filter-sterilized (0.22μm), and serial twofold dilutions were prepared in MH broth. The MIC was determined by the broth microdilution method in 96-well plates with MH broth (final volume 120μL per well), using an inoculum of 1×10^6 CFU/mL. The plates were incubated at 37°C for 16h, and the MIC was defined as the lowest concentration that completely inhibited visible bacterial growth. The assay was repeated at least three times.

2.6. Growth-curve assay

Ec032 was cultured to logarithmic phase and diluted to 1×10^6 CFU/mL. The bacterial suspension was incubated in 96-well plates with CRAMP-34 at 1/8×, 1/4×, 1/2×, 1×, 2× and 4×MIC at 37°C, and the OD600 was recorded every 1h for 24h to construct growth curves.

2.7. Biofilm assays

Biofilm biomass was quantified by crystal violet staining according to a microtiter-plate method, with minor modifications. For inhibition of biofilm formation, *Ec032* was co-incubated with CRAMP-34 at 1/8×, 1/4× and 1/2×MIC in 96-well plates at 37°C for 24h; the empty-vector supernatant served as the negative control. For eradication of preformed biofilms, 24h biofilms

were treated with CRAMP-34 at 1×, 2× and 4×MIC for 3h. After removal of the planktonic cells and washing with PBS, the biofilms were fixed with 99% methanol for 10min, air-dried and stained with crystal violet for 20min. The bound dye was solubilized with acetic acid and quantified at OD_{600} (Luo and Song 2021).

2.8. Membrane permeability assay

Membrane integrity was assessed by propidium iodide (PI) uptake as described previously, with minor modifications. *Ec032* cells were harvested, washed three times with PBS and incubated with CRAMP-34 (final concentrations of 1×, 2× and 4×MIC) for 30min at 37°C; PBS-treated cells served as the negative control. PI (final concentration 20μg/mL) was then added, and the cells were stained for 15min at room temperature in the dark. After washing with PBS, the cells were examined by fluorescence microscopy and the fluorescence intensity was analysed with ImageJ software (Wang et al. 2013).

2.9. DNA-binding assay

The interaction of CRAMP-34 with plasmid DNA was examined by agarose gel retardation. *E. coli* plasmid DNA (final concentration 200ng/mL) was mixed with CRAMP-34 at final concentrations of 1/8×, 1/4×, 1/2×, 1×, 2× and 4×MIC in TAE buffer and incubated at room temperature for 30min. The mixtures were separated on a 1.5% agarose gel, and the migration of the plasmid DNA was recorded (Yan et al. 2018).

2.10. Hemolytic activity assay

Hemolytic activity was evaluated using defibrinated sheep erythrocytes with minor modifications of the method of Oddo and Hansen (Oddo and Hansen 2017). Briefly, 250μL of CRAMP-34 solution at different concentrations was mixed with 250μL of 4% (v/v) sheep erythrocyte suspension and incubated at 37°C for 1h. The mixtures were then centrifuged, and the absorbance of the supernatants was measured at 540nm. PBS and 1% (v/v) Triton X-100 were used as the negative and positive controls (Sultana et al. 2021).

2.11. Stability assays

The stability of CRAMP-34 was evaluated by the agar well diffusion method, measuring the residual inhibition zone diameter against *Ec032* after the following treatments: (i) heating at 20, 40, 60, 80 or 100°C for 30min; (ii) incubation at pH 3, 4, 5, 6, 7, 8, 9, 10 or 11 (phosphate buffer, autoclaved); (iii) incubation with 50-200μM NaCl, $MgCl_2$, KCl, NH_4Cl, $CaCl_2$ or $FeCl_3$; (iv) up to eight freeze-thaw cycles (−80°C freezing followed by thawing at room temperature); and (v) incubation with trypsin, papain or pepsin at final concentrations of 10-1000μg/mL for 30min at 37°C. Untreated CRAMP-34 supernatant served as the control. Each experiment was performed independently in triplicate (Kim et al. 2014).

2.12. Statistical analysis

Data were analysed with Prism 8.0 (GraphPad Software, San Diego, CA, USA). Unpaired t-tests and one-way ANOVA were used to determine statistical significance. Differences were considered significant at $p<0.05$ (*), $p<0.01$ (**), $p<0.001$ (***) and $p<0.0001$ (****). All experiments were performed at least three times, and the results are expressed as the mean ± standard deviation.

3. Results

3.1. Construction and screening of the recombinant strain

The codon-optimized CRAMP-34 gene was synthesized and verified by Sanger sequencing (Fig. S1), then cloned into the pPIC9K vector to generate the recombinant plasmid pPIC9K-CRAMP-34 (Fig. S2). The plasmid was linearized with SacI, and correct linearization was confirmed by agarose gel electrophoresis (Fig. S3). Following transformation into *P. pastoris* GS115, transformants were initially selected on MD plates (Fig. S4A) and then screened for high-copy integrants on YPD medium containing increasing concentrations of G418 (Fig. S4B). Clones capable of growth on 3.0mg/mL G418 were recovered, and colony PCR confirmed the presence of the expression cassette in these transformants (Fig. S5), consistent with multi-copy genomic integration. A verified high-copy transformant was selected for all subsequent expression experiments (Kjeldsen et al. 2022).

3.2. Single-factor optimization of induction conditions

The inhibitory activity of the culture supernatant first increased and then decreased as the induction temperature was raised: activity was nearly absent at 22°C and 32°C, and the largest inhibition zone was observed at 26°C (Fig. 1A). Activity also increased with methanol concentration up to 2.5% (v/v) and declined slightly at higher concentrations (Fig. 1B), and increased with induction time up to 120h (Fig. 1C). On the basis of these single-factor profiles, the ranges selected for subsequent orthogonal optimization were 24–28°C, 2.0–3.0% methanol and 96–144h.

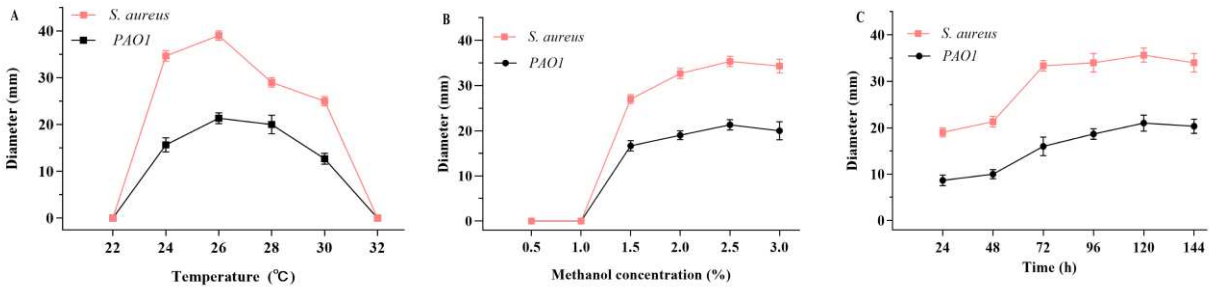


Fig. 1. Single-factor optimization of CRAMP-34 induction conditions in *P. pastoris* GS115. (A) Effect of induction temperature (22, 24, 26, 28, 30 and 32°C) on the antibacterial activity of the culture supernatant, expressed as inhibition zone diameter against *S. aureus* and *PAO1*. (B) Effect of methanol concentration (0.5, 1.0, 1.5, 2.0, 2.5 and 3.0%, v/v) on the antibacterial activity of the culture supernatant. (C) Effect of induction time (24, 48, 72, 96, 120 and 144h) on the antibacterial activity of the culture supernatant. Data are shown as the mean ± S.D of triplicate measurements.

3.3. Orthogonal optimization and verification

Based on the comprehensive score of the L9(3^4) orthogonal experiment (Table 1), range analysis indicated that the influence of the three factors ranked as induction time > methanol concentration > induction temperature. Analysis of variance confirmed that all three factors significantly affected the response ($p<0.05$; Table 2). The optimal combination was predicted as $A_1B_3C_3$, corresponding to 24°C, 3.0% (v/v) methanol and 144 h of induction. Three parallel validation runs under these conditions yielded a freeze-dried product of 5.66% (w/v) with a supernatant protein concentration of 2.06mg/mL (Table S1), and the low relative standard deviation confirmed the reproducibility of the optimized induction process.

Table 1. L9(3^4) orthogonal design and results for the optimization of CRAMP-34 induction conditions

Run	Temperature A (°C)	Methanol B (%)	Time C (h)	D	Inhibition zone (mm)	Protein (mg/mL)	Biofilm eradication (%)	Comprehensive score
1	1	1	1	1	25.89	2.46	33.33	78.79
2	1	2	2	2	29.78	2.25	32.54	80.51
3	1	3	3	3	29.67	2.28	53.23	93.92
4	2	1	2	3	26.89	2.07	43.36	82.01
5	2	2	3	1	29.00	2.65	26.01	79.93
6	2	3	1	2	29.44	2.71	21.91	78.52
7	3	1	3	2	26.44	2.50	39.61	83.90
8	3	2	1	3	18.33	2.05	38.47	68.66
9	3	3	2	1	19.78	2.35	55.10	84.27
K1	253.22	244.70	225.97	242.99				
K2	240.46	229.09	246.79	242.93				
K3	236.83	256.72	257.75	244.59				
k1	84.41	81.57	75.32	81.00				
k2	80.15	76.36	82.26	80.98				
k3	78.94	85.57	85.92	81.53				
R	5.46	9.21	10.59	0.55				

Table 2. Result of the variance analysis

Source of variation	Sum of squares (SS)	*df*	*F*	*F0.05*	*p-value*	Optimal level
A	49.43	2	84.07	19	<0.05	A_1
B	127.94	2	217.62	19	<0.05	B_3
C	173.75	2	295.54	19	<0.05	C_3
D	0.59	2				

3.4. Tricine-SDS-PAGE analysis of recombinant CRAMP-34 expression

Tricine-SDS-PAGE was performed to verify the expression of CRAMP-34 under the optimized induction conditions. As shown in Fig. 2, a single protein band of approximately 14 kDa was detected in the induced culture supernatant, consistent with the predicted molecular mass of the recombinant fusion peptide comprising the CRAMP-34 sequence, the α-factor signal peptide and the C-terminal 6×His tag, thereby confirming successful secretory expression of CRAMP-34 in *P. pastoris*.

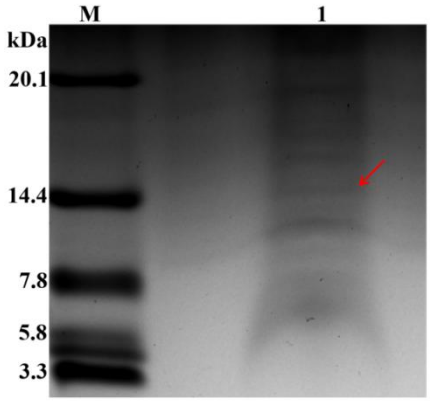


Fig. 2. Tricine-SDS-PAGE detection of CRAMP-34. Lane M: low range prestained protein ladder. Lane 1: The recombinant CRAMP-34 fusion protein, with a molecular weight of 14 kDa, was indicated by the arrow on the right.

3.5. Antibacterial activity and minimum inhibitory concentration

The optimized culture supernatant inhibited all five tested Gram-positive and Gram-negative strains, whereas the empty-vector supernatant showed no inhibitory activity against any of the tested bacteria (Table S2). The inhibition-zone assay revealed that activity was strongest against *A. lwoffii* and weakest against *P. aeruginosa*, with an overall ranking of *A. lwoffii* > *B. subtilis* > *S. aureus* > *E. coli* > *P. aeruginosa*; against *S. aureus* the inhibition zone was comparable to that of the ampicillin positive control, whereas against *A. lwoffii* the supernatant was more active than ampicillin. The MICs of the freeze-dried crude product ranged from 2mg/mL against *A. lwoffii* to 8 mg/mL against *P. aeruginosa*, *E. coli* and *B. subtilis* (Table 3), consistent with the inhibition-zone ranking (Fig. 3). These results demonstrated that recombinant CRAMP-34 exhibits broad-spectrum antibacterial activity.

Table 3. Minimum inhibitory concentrations of the recombinant CRAMP-34 freeze-dried product

Bacterial strain	MIC(mg/mL)
Staphylococcus aureus (ATCC25923)	4
Pseudomonas aeruginosa (ATCC27853)	8
Escherichia coli (ATCC25922)	8
Bacillus subtilis	8
Acinetobacter lwoffii	2

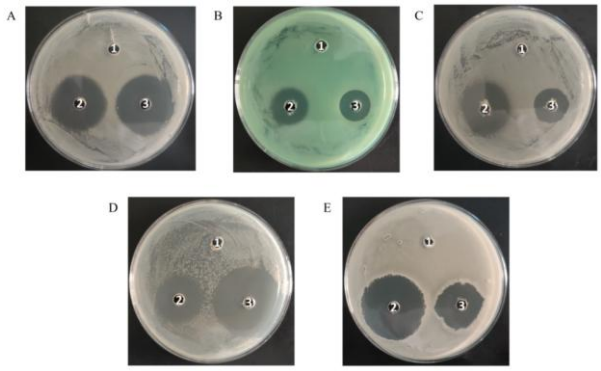


Fig. 3. The antibacterial activity of induced expression fermentation supernatant. the inhibition-zone ranking of (A): *S. aureus*; (B): *P. aeruginosa*; (C): *E. coli*; (D):*A. lwoffii*; (E):*B.subtilis.* 1: No load supernatant; 2: Positive control (ampicillin); 3: CRAMP-34 supernatant.

3.6. Effect on bacterial growth

In the growth-curve assay, CRAMP-34 inhibited Ec032 growth in a concentration-dependent manner (Fig. 4). Sub-MIC concentrations delayed entry into logarithmic phase, whereas concentrations at or above the MIC completely suppressed growth over the 24h monitoring period, indicating that CRAMP-34 exerts antibacterial effects in a concentration-dependent manner.

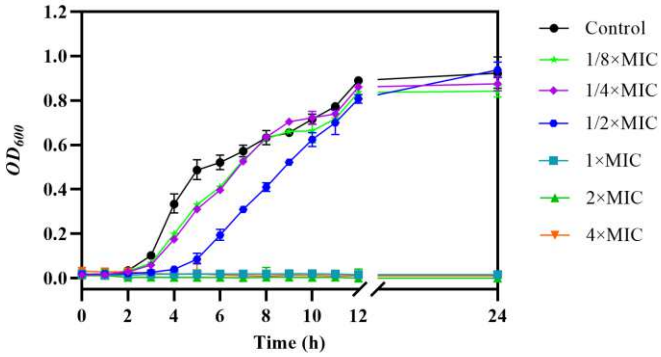


Fig. 4. Growth curves of *Ec032* treated with CRAMP-34 at different concentrations

3.7. Inhibition of biofilm formation and eradication of preformed biofilms

Crystal violet staining showed that co-incubation of *Ec032* with CRAMP-34 suppressed biofilm formation in a concentration-dependent manner, with 1/2×MIC concentrations producing pronounced reductions in biofilm biomass (Fig. 5A). In addition, treatment of preformed 24h biofilms with CRAMP-34 at concentrations above the MIC reduced biofilm biomass, although the eradication effect was less pronounced than the inhibition effect (Fig. 5B). These results indicated that CRAMP-34 is effective in both preventing biofilm development and reducing established biofilms.

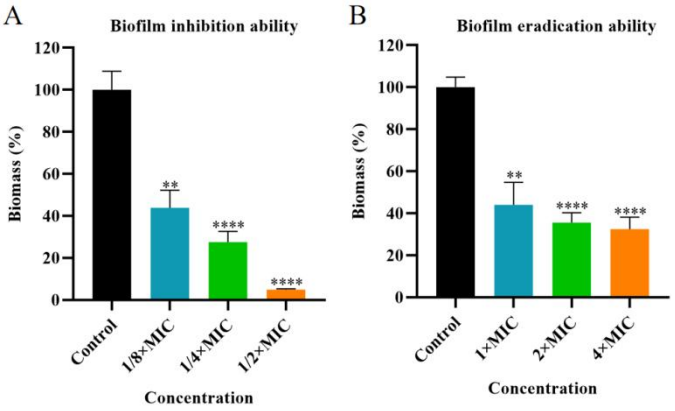


Fig. 5. Effect of optimized expression of CRAMP-34 products on the amount of *Ec032* biofilm.(A) Inhibition of biofilm formation.(B) Eradication of preformed biofilms.

3.8. Membrane permeability and DNA-binding activity

To explore the antibacterial mechanism, membrane permeability and DNA-binding activity were assessed. Propidium iodide uptake by *Ec032* increased significantly after CRAMP-34 treatment in a concentration-dependent manner, indicating permeabilization of the bacterial cytoplasmic membrane (Fig. 6). In the gel-retardation assay, migration of plasmid DNA was progressively retarded with increasing peptide concentration, demonstrating concentration-dependent binding of CRAMP-34 to plasmid DNA (Fig. 7). These findings suggest that membrane disruption and intracellular DNA interaction may contribute to the antibacterial activity of CRAMP-34.

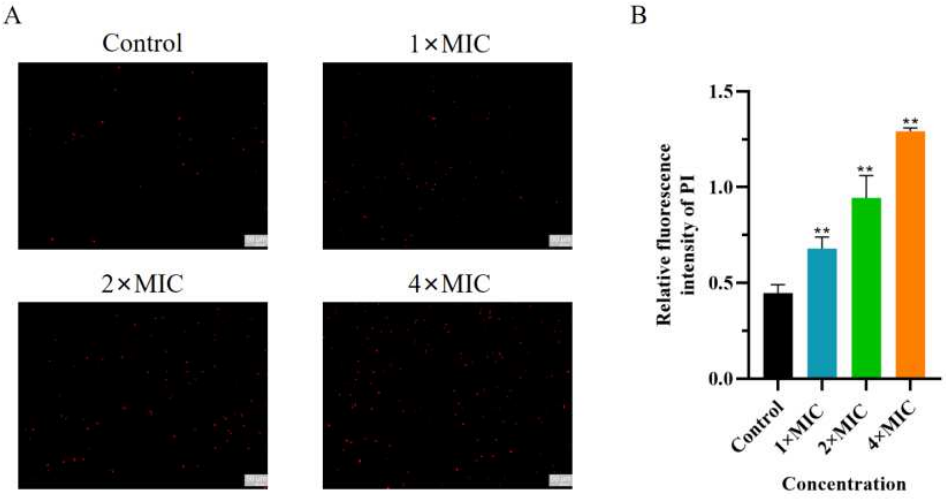


Fig. 6. Membrane permeabilization of *Ec032* by CRAMP-34, assessed by PI uptake.(A) The cells were observed by fluorescence microscopy.(B) the fluorescence intensity was analyzed with ImageJ software. Data are shown as the mean ± S.D. of triplicate measurements. $^{**}p < 0.01$, $^{***}p < 0.001$.

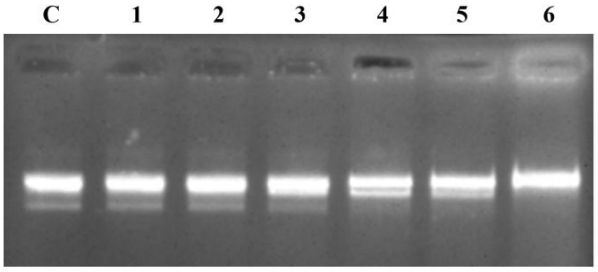


Fig. 7. DNA binding activity of CRAMP-34 products optimized at different concentrations.Lane C:Control; Lanes 1-6: DNA+CRAMP-34 at 1/8×, 1/4×, 1/2×, 1×, 2× and 4×MIC.

3.9. Hemolytic activity

CRAMP-34 showed only weak, concentration-dependent hemolysis of sheep erythrocytes (Fig. 8). Even at the highest concentration tested (256mg/mL), the hemolysis rate remained far below that of the 1% (v/v) Triton X-100 positive control. At the clinically relevant MIC range (2-8mg/mL), the hemolysis rate remained below 0.5%, indicating that CRAMP-34 exhibits high selectivity for bacterial membranes over mammalian erythrocyte membranes.

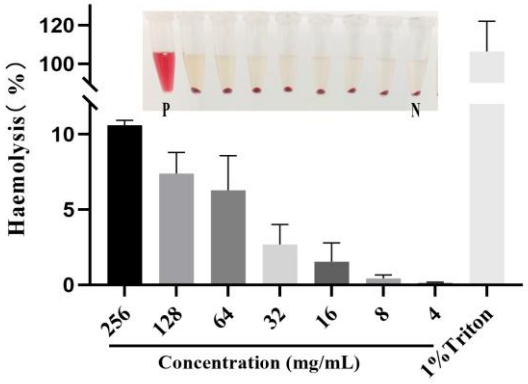


Fig. 8. Hemolytic activity of CRAMP-34 products against defibrinated sheep erythrocytes.PBS and 1% (v/v) Triton X-100 served as the negative (N) and positive (P) controls.

3.10. Stability of the recombinant peptide

The stability of CRAMP-34 was evaluated under various physicochemical conditions. As shown in Fig. 9, the antibacterial activity was not significantly affected by heating up to 100°C for 30min, by incubation with 50-200μM of the tested salts, or by up to eight freeze-thaw cycles. The peptide retained full activity under acidic conditions (pH 3-5), but activity declined progressively at neutral to alkaline pH. With respect to proteolytic digestion, pepsin had no effect on activity, whereas trypsin reduced activity in a concentration-dependent manner and papain reduced activity only at the highest concentration tested.

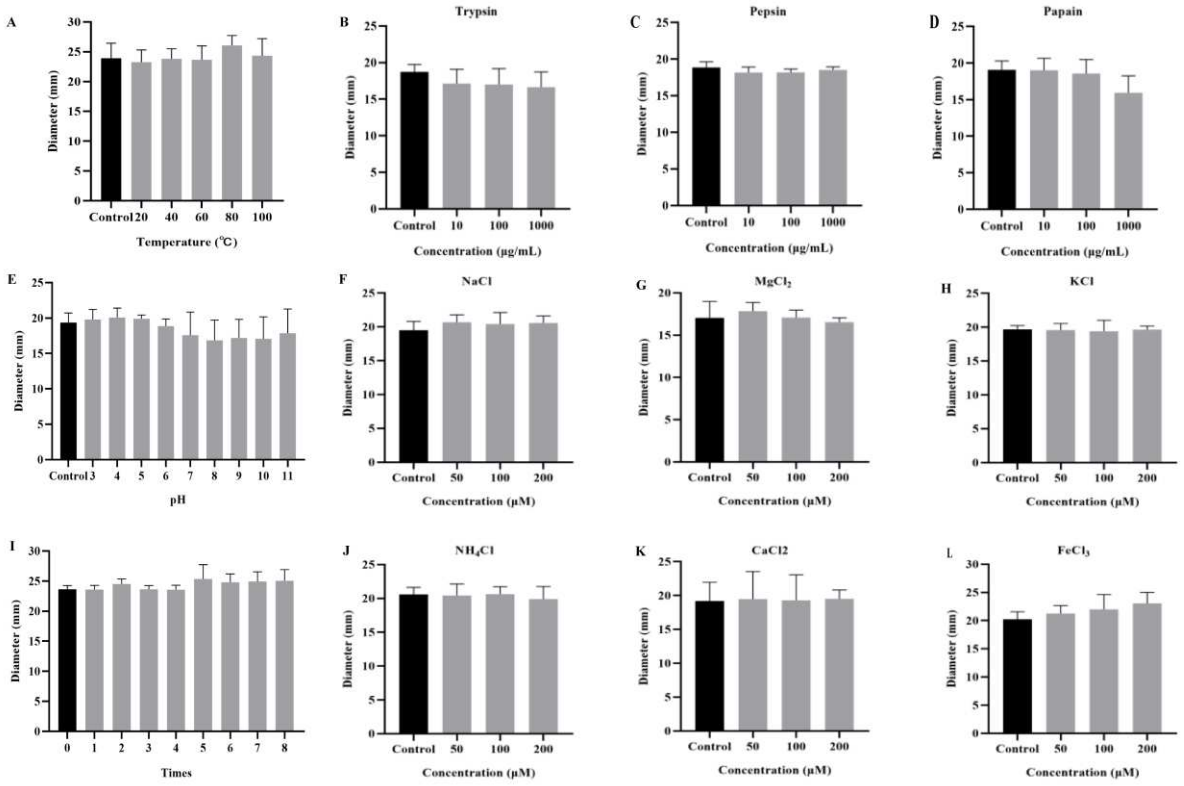


Fig. 9. Stability of CRAMP-34 under different physicochemical conditions. (A) Effect of heat treatment on antimicrobial activity of CRAMP-34. (B-D) Effects of different protease treatments on antimicrobial activity of CRAMP-34: (B) trypsin, (C) pepsin, (D) papain. (E) Effects of different pH conditions on antibacterial activity of CRAMP-34. (F-H) Effect of different salts on antimicrobial activity of CRAMP-34: (F) NaCl, (G) $MgCl_2$, (H) KCl. (I) Effects of repeated freeze-thaw cycles on antibacterial activity of CRAMP-34. (J-L) Effect of different salts on antimicrobial activity of CRAMP-34: (J) NH_4Cl, (K) $CaCl_2$, (L) $FeCl_3$.

4. Discussion

This study established a *P. pastoris* GS115-based secretory expression system for the mouse-derived cathelicidin CRAMP-34 and optimized the methanol-induced production process by combining single-factor experiments with an L9(3^4) orthogonal design. The optimized induction scheme-24°C, 3.0% (v/v) methanol replenished every 24h for a total of 144h, reproducibly yielded lyophilized crude-product yield at 5.66% (w/v) with a supernatant protein concentration of 2.06mg/mL in shake-flask culture. Functionally, the recombinant peptide showed broad antibacterial activity, strong anti-biofilm effects, membrane-permeabilizing and DNA-binding activity, low hemolysis, and good thermal, salt and freeze-thaw stability.

297 Optimal induction parameters vary substantially among recombinant AMPs, which largely arises
298 from peptide-specific differences in transcription efficiency, secretion competence, folding kinetics
299 and susceptibility to proteolytic degradation(Meng et al. 2017).For example, cathelicidin-BF was
300 optimally induced at 28°C with 1.0% methanol supplementation(Dong et al. 2023), whereas the
301 plant-derived peptide PaDef required 1.5% methanol for 72h at 28°C, and a dimeric LL37 variant
302 was produced with a distinct induction strategy in *P. pastoris*(Zhan et al. 2021).Such pronounced
303 inter-peptide differences reinforce that standard *P. pastoris* protocols cannot be directly transplanted
304 and that empirical optimization remains indispensable for each target AMP.

305 The optimal induction temperature of 24°C identified here is lower than the conventional 28-30°C
306 used for most *P. pastoris* secretory processes. Low-temperature induction has been reported to
307 reduce protein-folding stress and cell death and to limit the release of host proteases from lysed
308 cells, thereby improving the yield and integrity of secreted recombinant proteins(Jahic et al. 2003;
309 Macauley-Patrick et al. 2005).Consistent with this rationale, herring antifreeze protein expressed at
310 23°C markedly outperformed induction at 30°C(Li et al. 2001), and a recent optimization of
311 acidocin 4356 in Komagataella phaffii increased peptide synthesis by 34.12% when the induction
312 temperature was lowered from 30 to 21°C(Akbari et al. 2025). In the present orthogonal analysis,
313 induction time was the most influential factor (R = 10.59), followed by methanol concentration
314 (R=9.21), whereas temperature exerted a smaller effect (R=5.46), suggesting that the selected 24-
315 28°C range was already close to the response plateau. From a bioprocess perspective, the optimized
316 shake-flask conditions provide a promising basis for scale-up; transfer to a controlled fed-batch
317 bioreactor with precise regulation of methanol feeding, dissolved oxygen and pH, which strongly
318 shape the yield and quality of secreted proteins in *P. pastoris*(Bustos et al. 2022), is expected to
319 further improve production. In the present work, the yield of lyophilized crude product reached 5.66%
320 (w/v), demonstrating the reliability of the sequential single-factor-plus-orthogonal optimization
321 strategy. Nevertheless, cross-study yield comparisons must be interpreted cautiously, because crude
322 dry mass, purified peptide yield and biologically active peptide titre are not interchangeable metrics;

many published reports quantify HPLC-purified target peptides rather than total lyophilized crude product.

Recombinant CRAMP-34 inhibited all five tested Gram-positive and Gram-negative strains, with the strongest activity against *A. lwoffii* and the weakest against *P. aeruginosa*. The growth-curve data showed that 1/2×MIC concentrations delayed entry into logarithmic phase, whereas concentrations at or above the MIC completely suppressed growth over 24h, indicating concentration-dependent inhibition of bacterial growth.The anti-biofilm profile of CRAMP-34 is particularly noteworthy. Co-incubation with 1/2×MIC reduced biofilm formation by 95%, and 4×MIC eradicated 68% of pre-formed 24h biofilms. AMPs can suppress biofilm formation by interfering with bacterial adhesion and quorum-sensing pathways and can disperse mature biofilms by depolarizing membranes and disrupting extracellular polymeric substances, including extracellular DNA(Flemming and Wingender 2010). The pronounced inhibition observed at 1/2×MIC is functionally relevant, because sub-inhibitory doses are commonly encountered in vivo and would be expected to reduce the selective pressure for resistance.

The PI-uptake and gel-retardation assays support two potential effects: permeabilization of the bacterial cytoplasmic membrane and interaction with plasmid DNA, as proposed for other cationic AMPs, including the human cathelicidin LL-37, that act on both membrane and intracellular targets(Brogden 2005; Xhindoli et al. 2016). Such multi-target mechanisms are considered advantageous because they make the emergence of bacterial resistance substantially more difficult than against single-target antibiotics(Hilchie et al. 2013),The low hemolytic activity of CRAMP-34 is favorable for further development. Even at 256mg/mL, the hemolysis rate was only 10.7%, and within the MIC range the hemolysis remained below 0.5%. This high selectivity likely arises from differences in membrane composition: bacterial membranes are enriched in anionic phospholipids that promote electrostatic recruitment of cationic peptides, whereas mammalian erythrocyte membranes are zwitterionic and contain cholesterol, which stabilizes the lipid bilayer and resists peptide insertion(Zasloff 2002).

CRAMP-34 retained full activity after heating to 100°C, exposure to 50-200μM salts, repeated freeze-thaw cycles and pepsin digestion, properties that are desirable for downstream processing, dry storage and passage through the gastric compartment. However, activity declined under alkaline conditions and after trypsin treatment and was reduced by high-dose papain. Trypsin sensitivity is a common limitation of cationic peptides rich in basic residues and may shorten the in vivo half-life in protease-rich tissues; engineering strategies such as N-terminal acetylation, peptide cyclization or fusion with protease-stabilizing partners have been shown to mitigate protease susceptibility for related AMPs and should be explored for CRAMP-34 derivatives(Li et al. 2021). The high thermal stability, wide pH tolerance and pepsin resistance of CRAMP-34 support its suitability for oral delivery applications, and AMP-based feed additives have shown beneficial effects on growth performance and intestinal health in weaned piglets(Zhang et al. 2021), further supporting the potential of CRAMP-34 as a feed-additive candidate.

All antibacterial and stability assays in this study were performed using unpurified preparations (induced culture supernatant or lyophilized crude product), and the reported MIC values therefore refer to the mass concentration of the lyophilized powder rather than that of purified CRAMP-34. The reproducible, concentration-dependent effects, together with the empty-vector control, indicate that the observed activities are attributable to recombinant CRAMP-34. Nevertheless, residual medium components and host-derived proteins in the crude preparations may affect the measurements, and the absolute MIC values should therefore be interpreted with caution and are not directly comparable to literature values obtained with purified peptides.

In summary, we established an efficient *Pichia pastoris* GS115 platform for recombinant CRAMP-34 production. Combined single-factor and orthogonal experiments yielded optimized induction parameters with a freeze-dried product yield of 5.66%. CRAMP-34 showed broad antibacterial and antibiofilm effects, relying on membrane permeabilization and DNA binding. The peptide maintained bioactivity after heat, salt, freeze-thaw and acidic treatments. This study demonstrates

CRAMP-34's potential as an antibiotic alternative for feed additives, and the established expression pipeline provides a useful reference for large-scale AMP production in methylotrophic yeast.

References:

Akbari A, Talaee M, Mir-Derikvand M et al. (2025) Heterologous expression and optimization of the antimicrobial peptide acidocin 4356 in komagataella phaffii to target pseudomonas aeruginosa. Appl Microbiol Biot 109:231 doi:10.1007/s00253-025-13584-1

Barone GD, Emmerstorfer-Augustin A, Biundo A et al. (2023) Industrial production of proteins with pichia pastoris-komagataella phaffii. Biomolecules 13:441 doi:10.3390/biom13030441

Bhattacharjya S, Zhang Z, Ramamoorthy A (2024) Ll-37: structures, antimicrobial activity, and influence on amyloid-related diseases. Biomolecules 14:320 doi:10.3390/biom14030320

Brogden KA (2005) Antimicrobial peptides: pore formers or metabolic inhibitors in bacteria? Nature Reviews. Microbiology 3:238-250 doi:10.1038/nrmicro1098

Bustos C, Quezada J, Veas R et al. (2022) Advances in cell engineering of the komagataella phaffii platform for recombinant protein production. Metabolites 12:346 doi:10.3390/metabo12040346

Dong X, Shan H, Wang S et al. (2023) High expression of antimicrobial peptides cathelicidin-bf in pichia pastoris and verification of its activity. Front Microbiol 14:1153365 doi:10.3389/fmicb.2023.1153365

Flemming H, Wingender J (2010) The biofilm matrix. Nature Reviews. Microbiology 8:623-633 doi:10.1038/nrmicro2415

Garrigós-Martínez J, Vuoristo K, Nieto-Taype MA et al. (2021) Bioprocess performance analysis of novel methanol-independent promoters for recombinant protein production with pichia pastoris. Microb Cell Fact 20:74 doi:10.1186/s12934-021-01564-9

Hilchie AL, Wuerth K, Hancock REW (2013) Immune modulation by multifaceted cationic host defense (antimicrobial) peptides. Nat Chem Biol 9:761-768 doi:10.1038/nchembio.1393

Jahic M, Wallberg F, Bollok M et al. (2003) Temperature limited fed-batch technique for control of proteolysis in pichia pastoris bioreactor cultures. Microb Cell Fact 2:6 doi:10.1186/1475-2859-2-6

Kim H, Jang JH, Kim SC, Cho JH (2014) De novo generation of short antimicrobial peptides with enhanced stability and cell specificity. The Journal of Antimicrobial Chemotherapy 69:121-132 doi:10.1093/jac/dkt322

401 Kjeldsen A, Kay JE, Baxter S et al. (2022) The fluorescent protein ilov as a reporter for screening of high-yield
402 production of antimicrobial peptides in pichia pastoris. Microb Biotechnol 15:2126-2139 doi:10.1111/1751-
403 7915.14034

404 Li D, Yang Y, Li R et al. (2021) N-terminal acetylation of antimicrobial peptide l163 improves its stability against
405 protease degradation. Journal of Peptide Science : An Official Publication of the European Peptide Society
406 27:e3337 doi:10.1002/psc.3337

407 Li Z, Xiong F, Lin Q et al. (2001) Low-temperature increases the yield of biologically active herring antifreeze
408 protein in pichia pastoris. Protein Expres Purif 21:438-445 doi:10.1006/prep.2001.1395

409 Luo Y, Song Y (2021) Mechanism of antimicrobial peptides: antimicrobial, anti-inflammatory and antibiofilm
410 activities. International Journal of Molecular Sciences 22:11401 doi:10.3390/ijms222111401

411 Macauley-Patrick S, Fazenda ML, McNeil B, Harvey LM (2005) Heterologous protein production using the
412 pichia pastoris expression system. Yeast (Chichester, England) 22:249-270 doi:10.1002/yea.1208

413 Meng D, Zhao J, Ling X et al. (2017) Recombinant expression, purification and antimicrobial activity of a novel
414 antimicrobial peptide padef in pichia pastoris. Protein Expres Purif 130:90-99 doi:10.1016/j.pep.2016.10.003

415 Mohammadzadeh R, Karbalaei M, Soleimanpour S et al. (2021) Practical methods for expression of recombinant
416 protein in the pichia pastoris system. Current Protocols 1:e155 doi:10.1002/cpz1.155

417 Oddo A, Hansen PR (2017) Hemolytic activity of antimicrobial peptides. Methods in Molecular Biology (Clifton,
418 N.J.) 1548:427-435 doi:10.1007/978-1-4939-6737-7_31

419 Pontes JTCD, Toledo Borges AB, Roque-Borda CA, Pavan FR (2022) Antimicrobial peptides as an alternative for
420 the eradication of bacterial biofilms of multi-drug resistant bacteria. Pharmaceutics 14:642
421 doi:10.3390/pharmaceutics14030642

422 Roca-Pinilla R, Lisowski L, Arís A, Garcia-Fruitós E (2022) The future of recombinant host defense peptides.
423 Microb Cell Fact 21:267 doi:10.1186/s12934-022-01991-2

424 Sultana A, Luo H, Ramakrishna S (2021) Antimicrobial peptides and their applications in biomedical sector.
425 Antibiotics (Basel, Switzerland) 10:1094 doi:10.3390/antibiotics10091094

Svensson D, Nilsson B (2025) Human antimicrobial/host defense peptide ll-37 may prevent the spread of a local infection through multiple mechanisms: an update. Inflammation Research : Official Journal of the European Histamine Research Society ... [Et Al.] 74:36 doi:10.1007/s00011-025-02005-8

Talapko J, Meštrović T, Juzbašić M et al. (2022) Antimicrobial peptides-mechanisms of action, antimicrobial effects and clinical applications. Antibiotics (Basel, Switzerland) 11:1417 doi:10.3390/antibiotics11101417

Wang K, Dang W, Yan J et al. (2013) Membrane perturbation action mode and structure-activity relationships of protonectin, a novel antimicrobial peptide from the venom of the neotropical social wasp agelaia pallipes pallipes. Antimicrob Agents Ch 57:4632-4639 doi:10.1128/AAC.02311-12

Wang Y, Song M, Chang W (2024) Antimicrobial peptides and proteins against drug-resistant pathogens. Cell Surface (Amsterdam, Netherlands) 12:100135 doi:10.1016/j.tcsw.2024.100135

Xhindoli D, Pacor S, Benincasa M et al. (2016) The human cathelicidin ll-37--a pore-forming antibacterial peptide and host-cell modulator. Biochimica Et Biophysica Acta 1858:546-566 doi:10.1016/j.bbamem.2015.11.003

Xie F, Zan Y, Zhang X et al. (2020) Differential abilities of mammalian cathelicidins to inhibit bacterial biofilm formation and promote multifaceted immune functions of neutrophils. International Journal of Molecular Sciences 21:1871 doi:10.3390/ijms21051871

Yan J, Liang X, Liu C et al. (2018) Influence of proline substitution on the bioactivity of mammalian-derived antimicrobial peptide nk-2. Probiotics Antimicro 10:118-127 doi:10.1007/s12602-017-9335-1

Zasloff M (2002) Antimicrobial peptides of multicellular organisms. Nature 415:389-395 doi:10.1038/415389a

Zeth K, Sancho-Vaello E (2021) Structural plasticity of ll-37 indicates elaborate functional adaptation mechanisms to bacterial target structures. International Journal of Molecular Sciences 22:5200 doi:10.3390/ijms22105200

Zhan N, Zhang L, Yang H et al. (2021) Design and heterologous expression of a novel dimeric ll37 variant in pichia pastoris. Microb Cell Fact 20:143 doi:10.1186/s12934-021-01635-x

Zhang L, Guo T, Zhan N et al. (2021) Effects of the antimicrobial peptide wk3 on diarrhea, growth performance and intestinal health of weaned piglets challenged with enterotoxigenic escherichia coli k88. Food Nutr Res 65:10-29219 doi:10.29219/fnr.v65.3448

Zhang M, Liang W, Gong W et al. (2019) The critical role of the antimicrobial peptide ll-37/ cramp in protection of colon microbiota balance, mucosal homeostasis, anti-inflammatory responses, and resistance to carcinogenesis. Crit Rev Immunol 39:83-92 doi:10.1615/CritRevImmunol.2019030225

Zhang Q (2025) Antimicrobial peptides: from discovery to developmental applications. Appl Environ Microb 91:e211524 doi:10.1128/aem.02115-24

Supplementary Files

This is a list of supplementary files associated with this preprint. Click to download.

- Supplementarydata.docx